Nanomechanical Devices Based on DNA**

Christof M. Niemeyer* and Michael Adler

Biomolecular compounds, such as proteins and nucleic acids, which are evolutionary optimized, with respect to specificity of binding to their target structure as well as to functionality, for distinct biochemical transformation and translocation, are currently explored as building blocks in the "bottom-up" self-assembly of nanometer-scale functional devices.[1] So far, applications include the organization of metal and semiconductor nanoclusters,[2] numerous bioanalytical techniques,[1] as well as biomolecular electronics[3] and nanomechanical devices. While the development of the latter was, in past years, mainly focused on motor proteins, such as actin, kinesin, and myosin,[4] nowadays an increasing number of reports are being devoted to the construction of nanomechanical devices from DNA. This biomolecule plays an outstanding role in the development of artificial biomolecular hybrid elements, since the specificity of simple A-T and G-C base pairing as well as its robust physicochemical nature allows for the fabrication of nanostructured molecular scaffolding and surface architecture,[5] and to selectively position proteins,[6] inorganic colloidal components,[2] carbohydrates,[7] organometallics,[8] and reactive chemical compounds[9] on the nanometer length scale.

Another interesting property of the DNA double helix is its intrinsic susceptibility to external stimuli mediated by small molecules or ions, which opens up ways to fabricate nanomechanical devices. For example, the contour length and the flexibility of a DNA molecule can be effectively altered by use of intercalators, such as acridinium or ethidium bromide derivatives, which bind in between the stacked nucleobases of the double helix and thereby significantly increase the DNA contour length.[10] Seeman and co-workers made use of this phenomenon: They reported on the induced change in torque of a circular DNA molecule containing a partially mobile branched DNA junction on intercalation of ethidium bromide as a potential supercoiling motion for nanomechanical elements.[11]

More recently, the Seeman group established an elegant means to utilize electrostatic interaction of Co^{3+} ions for switching a DNA device comprised of two rigid DNA double-crossover motifs. The latter were covalently linked to each other by a short $d(CG)_{10}$ proto-Z sequence which is capable of changing its conformation from a right-handed B- to a left-handed Z-DNA double helix (Figure 1 A).[12] The conformational change leads to a spatial separation of two fluorescent labels, attached to each of the two double-crossover moieties, which can be measured by fluorescence resonance energy transfer (FRET).

In a different approach, the increase in concentration of Mg^{2+} ions was used to trigger a supercoiling of two DNA strands within supramolecular aggreates comprised of biotinylated DNA and streptavidin (STV).[13] The twisting of the DNA strands leads to a decrease in the distance between adjacent STV particles (Figure 1 B). Potential applications of such structural changes might include the fabrication of ion-dependent molecular switches within nanomaterials, for example, to control nanoparticle spacing and to regulate the accessibility of the DNA to enzymes.

Whilst the above examples concern the more or less gradual conformational switching of molecular devices by small molecule effectors,[14] a different strategy relies on DNA motifs whose conformation is sharply switched by intermolecular hybridization with complementary nucleic acids. The developments of "molecular beacons" can be considered as a simple example of such a process, thus allowing the utilization of hybridization-induced changes in DNA conformation for the macroscopic detection of intermolecular binding.[15] DNA beacons are single-stranded DNA (ssDNA) molecules which, as a result of their nucleotide sequence, form an intramolecular hairpin-loop structure (Figure 2 A). Both ends are chemically modified with a fluorophore F and a dye Q, the latter of which effectively quenches the fluorescence of F by its spatial proximity. Upon hybridization with nucleic acid targets containing a sequence stretch complementary to the loop region of the beacon, Q is spatially removed from F, which leads to a strong enhancement in fluorescence. Since its first description, this simple yet powerful principle has been applied to numerous applications ranging from homogeneous hybridization analysis, to real-time polymerase chain reaction (PCR) and detection of single nucleotide polymorphism.[16]

Recently, a new class of molecular beacons has been introduced, in which the organic quencher dye Q was replaced by a gold metal cluster (Figure 2 C).[17] This hybrid construct was synthesized from a 3′-amino-5′-thiol-modified ssDNA oligomer by subsequent coupling with an amino-reactive fluorophore and with commercially available 1.4-nm gold clusters containing a single maleimido group in their ligand shell. The performance of the hybrid molecular beacon was optimized by determining the quenching efficiency (QE), that is, the difference in fluorescence between the open duplex and the intramolecularly closed beacon, for several dyes. The best QE value of about 99.5 % was obtained for rhodamine 6G, which indicates that the fluorescence signal of the beacon increases about 200-fold upon hybridization with the complementary target. Consequently, the gold-oligomer-dye hybrids were applied to the detection of single mismatches in DNA. Competitive hybridization assays revealed that the ability to

[*] Prof. Dr. C. M. Niemeyer
Universität Dortmund, Fachbereich Chemie
Biologisch-Chemische Mikrostrukturtechnik
Otto-Hahn Strasse 6, 44227 Dortmund (Germany)
Fax: (+49) 231-755-5048
E-mail: cmn@chemie.uni-dortmund.de
Dr. M. Adler
Chimera Biotec GmbH
Emil-Figge Strasse 76a, 44227 Dortmund (Germany)

[**] We thank Prof. D. Blohm for his continuous support.

  1433-7851/02/4120-3779 $ 20.00+.50/0

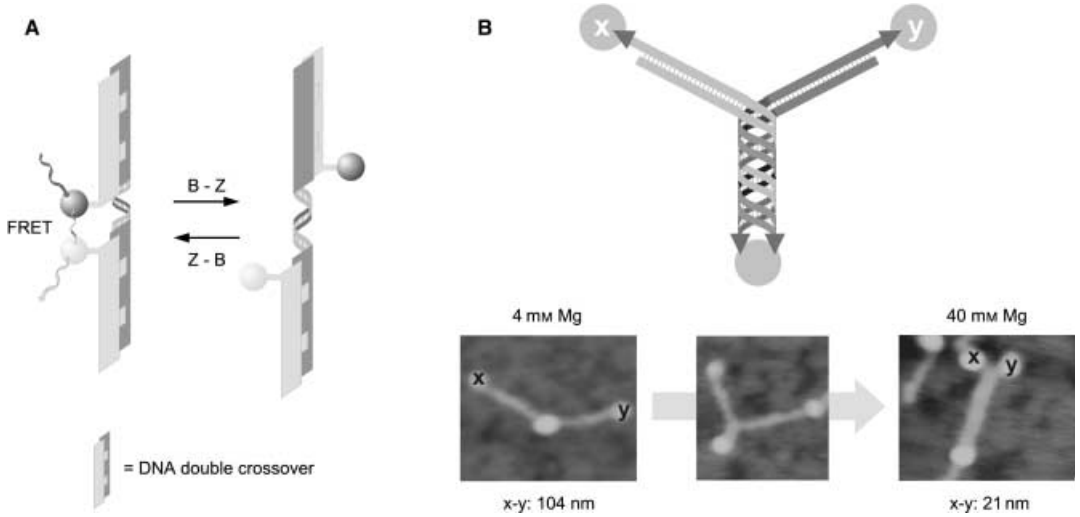

Figure 1. Electrostatic switching of DNA devices. A) A nanomechanical device consisting of two rigid double-crossover structures connected by a double-helical DNA fragment. The presence of $[CoCl_3(NH_3)_6]$ triggered the conformational change of the double helix from a right-handed B to a left-handed Z helix, thus separating two adjacent fluorophores coupled to each of the double-crossover moieties. The rotational movement was detected by the interruption of the FRET signal occurring between the two fluorophores in the B-DNA conformation and was reversed by eliminating the $[CoCl_3(NH_3)_6]$ from the solution. B) Aggregates consisting of STV and bis-biotinylated DNA change their conformation in the presence of Mg^{2+} ions. AFM images of aggregates comprised of three STV and two DNA molecules are shown. The Mg^{2+}-induced supercoiling of the DNA strands leads to alterations in the STV–STV distance between "x" and "y" from 104 to 21 nm.

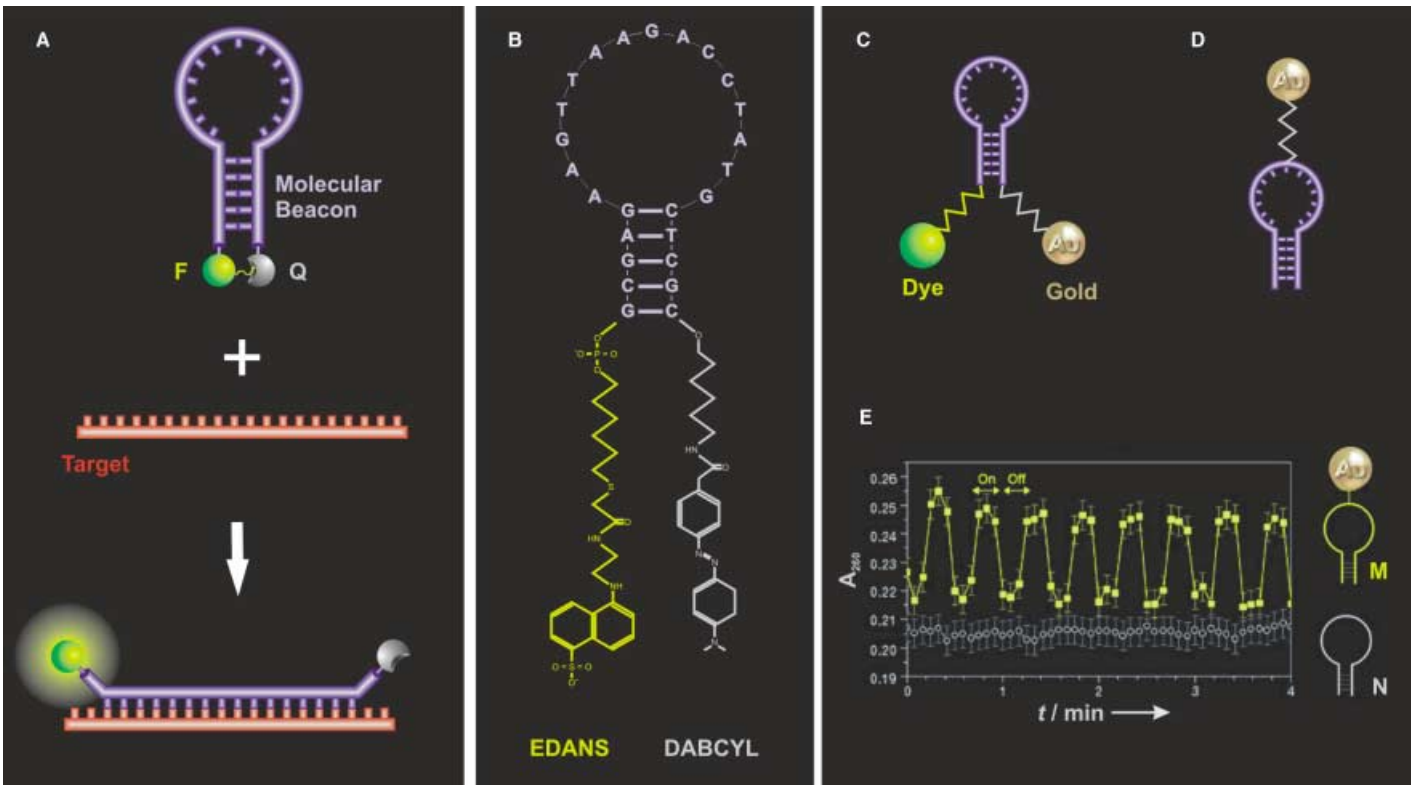

Figure 2. Nanomechanical motion of nucleic acid motifs with a hairpin structure. A) Conventional molecular beacons.[15] B) Example of fluorescent dyes attached to a DNA hairpin molecule. C) Molecular beacon containing a 1.4-nm gold nanocrystal as a quencher.[17] D) Electronic switching of DNA hybridization.[18] The hairpin molecule M is self-complementary at the ends for seven bases, with a primary amine in the loop to which a 1.4-nm gold nanocrystal is covalently linked. E) The absorbance of a solution of M at 260 nm is plotted as a function of time in which the radio-frequency magnetic field is switched on and off. The increase in absorbance reflects the denaturation of the DNA double helix. For control purposes, a solution of hairpin molecule N, which lacks the gold nanocrystal, was analyzed under similar conditions. Adapted with kind permission from ref. [18].

detect single base mutations is about eightfold greater than with conventional molecular beacons while the sensitivity of detection is enhanced up to 100-fold.[17] Nonetheless, limitations in the applicability of such hybrid constructs in routine diagnostics are currently a consequence of the limited physicochemical stability of the metal clusters, their ligand

  1433-7851/02/4120-3780 $ 20.00+.50/0

shell, and the chemical linkage between the clusters and the DNA.

Gold nanoparticle/DNA molecular beacon conjugates have recently been exploited for the remote electronic control of DNA hybridization (Figure 2D).[18] By inductively coupling a radio-frequency magnetic field (RFMF) with a frequency of 1 GHz to the 1.4-nm metal nanocrystal, which functions as an antenna in the DNA constructs, the local temperature of the bound DNA is increased, thereby inducing denaturation while leaving surrounding molecules relatively unaffected. The switching is fully reversible (Figure 2E). Although inductive heating has already been applied to macroscopic samples, as well as in the treatment of cancer cells with magnetic-field-induced excitation of biocompatible superparamagnetic nanoparticles,[19] the use of gold nanocrystal/DNA conjugates should allow extension of this concept. For example, complex operations, such as gene regulation, biomolecular assembly, and enzymatic activity, of distinct portions of nucleic acids or proteins might be controlled, while the rest of the molecule and neighboring species would remain unaffected. Moreover, because the addressing is not optical, this technology would even be applicable in highly scattering media.

Conformational changes induced by intermolecular hybridization of complementary DNA molecules were also translated into a nanomechanical response by using an array of eight microfabricated cantilevers.[20] Each individual cantilever contained a different capture oligonucleotide, and the hybridization with target oligomers led to differences in surface stress between cantilevers functionalized with complementary or noncomplementary DNA oligomers. Hybridization experiments revealed that a single-base mismatch between two 12-mer oligonucleotides were clearly detectable. Recently, such cantilever-based nanomechanical sensor devices were applied in the detection of cancer antigens[21] and single nucleotide polymorphisms.[22] Moreover, systematic DNA hybridization experiments revealed that the origin of the motion of the cantilever lies in the interplay between changes in configurational entropy and intermolecular energetics induced by specific biomolecular interactions.[23]

Intermolecular DNA hybridization also plays a key role in the concept of "fueling" DNA nanomechanical devices by strand-exchange reactions. A first example of this type was reported by Yurke et al.[24] They constructed a molecular tweezer from three oligonucleotides, one of which is doubly labeled with a 3′-TAMRA (carboxytetramethylrhodamine) and a 5′-TET (tetrachlorofluorescein) fluorogenic group (strand T_a in Figure 3A). Strands T_b and T_c are partially complementary to strand T_a and form two rigid double helices and a four-base-hinge single-stranded region within the intermolecular tweezer complex. In this conformation, termed as the machine's "rest state", the remaining two unhybridized 24-base portions of 42-mer strands T_b and T_c dangle floppily from the ends of the tweezer. In the rest state, the two fluorophores of strand T_a are spatially separated and no intermolecular resonant energy transfer from TET to TAMRA, and thus, no quenching of TET fluorescence occurs. The tweezer is operated by the addition of fueling strands F_c and F_o (Figure 3A). Closing strand F_c is comprised of three regions, two of which are 24-mers fully complementary to the dangling ends of strands T_b and T_c, and the third region is an 8-mer overhang at which interaction with opening strand F_o begins. Addition of F_c pulls the ends of the tweezer together by intermolecular hybridization (Figure 3A), which leads to a decrease of the TET fluorescence by a factor of six. The tweezer is re-opened by addition of F_o, which is fully complementary to F_c. Starting with intermolecular hybridization of F_o and F_c at the 8-mer overhang stretch, F_c is displaced from the tweezer by branch-migration and leads to the formation of the F_cF_o duplex as a "waste" product. The opening/closing process is fully reversible, and the switching time for the machine is less than 20 s with second-order rate constants for opening and closing being approximately equal. Interestingly, thermodynamic calculations suggest a closing force of the tweezer of about 15 pN, which is at the upper end of the range of measured forces exerted by single-group kinesin and myosin motors.[24]

The above scheme has recently been modified by Li and Tan.[25] They constructed a 17-mer DNA nanomotor which can adopt an intramolecular tetraplex (TE) conformation through the formation of two layers of intramolecular G-quartetts (Figure 3B). In this shrunken state, the fluorophore F and the quencher Q are in spatial proximity, and consequently the nanomotor is in its dark state. Hybridization with complementary fueling oligomer F_a results in the nanomotor extending into a duplex (DU) conformation, thereby separating the two ends from each other, and thus, the fluorescence intensity increases approximately fourfold. The nanomotor shrinks back to the TE when strand F_a is displaced by hybridization with complementary strand F_b, thereby producing a waste DNA duplex F_aF_b. Addition of F_a starts a new extending/shrinking cycle. Cycling of the nanomotor in homogeneous solution revealed that the process is almost fully reversible. Moreover, nanomotors were immobilized at a surface and the fully reversible cycling of the extending/shrinking motion suggested that such devices might be useful for pulling together and pushing apart two nanoelements in a future nanosystem. Theoretical calculations allowed the estimatation of the shrinking force ($F_{sh} = 2.2$ pN) and the extending force ($F_{ex} = 20.7$ pN), which are in the same order of magnitude or about tenfold greater, respectively, than those of kinesin and myosin protein nanomotors.

Seeman and co-workers have recently described a highly sophisticated DNA nanomechanical device[26] which demonstrates that ssDNA fragments can be used to control and fuel a DNA device cycle by inducing the interconversion between two topological motifs—paranemic crossover (PX) DNA and its topoisomer (JX_2) DNA (Figure 3C). The two crossover motifs can be converted into each other by removal of internal strands with the aid of biotinylated fueling strands, which allow their elimination with streptavidin-coated magnetic beads. The cycling of the PX/JX_2 device was demonstrated by gel electrophoresis as well as by atomic force microscopy. The latter was conducted by modifying the PX/JX_2 device with a regular array of topographic markers in the form of half-hexagon motifs formed by DNA double helices (Figure 3D). Switching of the DNA device from the PX to the JX_2 state

  1433-7851/02/4120-3781 $ 20.00+.50/0

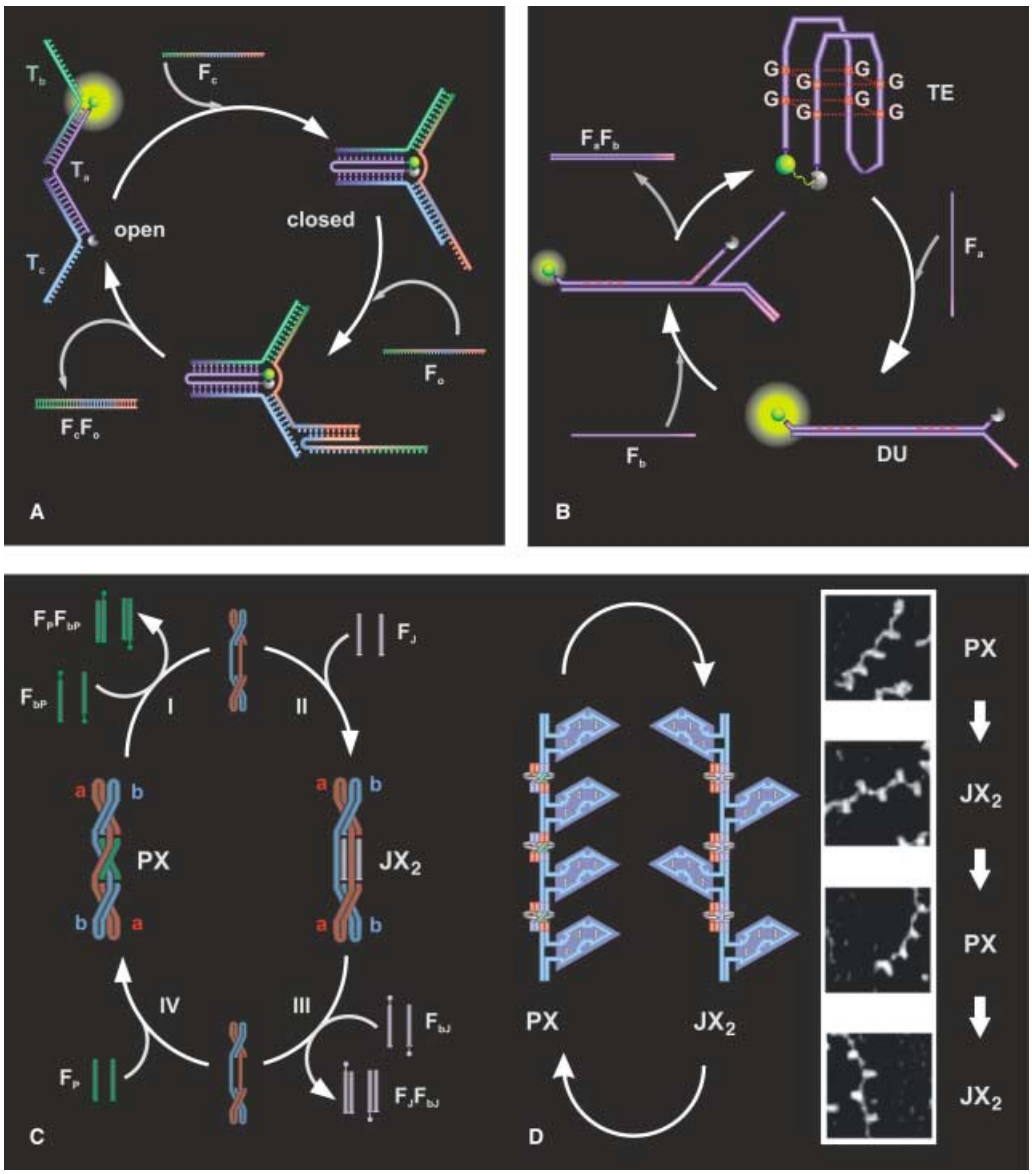

Figure 3. Control of nanomechanical motion of DNA motifs by "fueling" with single-stranded DNA molecules. A) The molecular tweezer structure comprised of three oligonucleotides T_a, T_b, and T_c is opened and closed by the addition of fueling oligonucleotides, which close the tweezer (F_c) and re-open it (F_o) by strand exchange.[24] B) Schematic drawing of the DNA nanomotor cycled between the intramolecular TE and intermolecular DU conformation by means of fueling oligomers F_a and F_b.[25] C) Schematic drawing of the PX/JX_2 device.[26] The PX motif consists of two helical domains formed by four strands that flank a central dyad axis. The JX_2 motif lacks two crossovers in the middle. Two strands are drawn in red and two in blue, and the letters a and b show that strands at the bottom of the JX_2 motif are rotated 180° relative to the PX motif. The device is operated by the addition of biotinylated fuel strands F_{bP} (green) which remove complementary strands F_P from the PX motif in process I. The unstructured intermediate is converted into the JX_2 motif by the addition of the purple set of strands F_J in process II. The JX_2 molecule is converted into the unstructured intermediate by the addition of biotinylated pale purple fuel strands F_{bJ} in process III. The two intermediates are identical. The cycle is completed by the addition of the green set of strands F_P in process IV, thus restoring the PX device. D) Experimental evidence for the operation of the PX/JX_2 device. A one-dimensional array of half hexagons is joined by PX/JX_2 motifs. The half-hexagons, each of which consists of three edge-sharing DNA triangles, are used as topographic markers that are traceable by AFM, as shown in the right panel. The images represent four steps of the operation of the device, originating from PX state (top) to JX_2 to PX, and back to JX_2 state (bottom). The PX linear arrays are clearly in the *cis* arrangement while the JX_2 linear arrays are in the *trans* arrangement. All images show an area of 200 × 200 nm. Adapted with kind permission from ref. [26].

leads to conversion of the arrangement of the half-hexagons from a *cis* to a *trans* configuration.

These examples indicate how various kinds of nanomechanical motion of DNA motifs can be realized, and range from an opening/closing of a DNA tweezer, to a crawling shrinking/extention linear movement and a relatively simple rotation around a central DNA axis. It seems likely that the the next steps will concern the implementation of these mechanical actions to the construction of hybrid devices which contain functional moieties, such as ribozyme motifs, proteins, colloids, or low-molecular-weight components, tethered to the mechanical entity. Such devices might be applied to investigate the interaction of chemically active components attached to the ends of a tweezer or to alternatively hide and reveal target groups attached to the DNA. DNA strands that act as fuel might also be used as information carriers to

  1433-7851/02/4120-3782 $ 20.00+.50/0

coordinate components of a complex machine or to carry signals between machines.[24] In regard to the latter, it should be noted that Benenson et al. have recently demonstrated a programmable computing machine made of biomolecular components, namely, DNA and DNA-manipulating enzymes, which is capable of autonomously solving computational problems.[27] One may anticipate plenty of exciting new developments in this young field of research.

[1] C. M. Niemeyer, *Angew. Chem.* **2001**, *113*, 4254 – 4287; *Angew. Chem. Int. Ed.* **2001**, *40*, 4128 – 4158.

[2] J. J. Storhoff, C. A. Mirkin, *Chem. Rev.* **1999**, *99*, 1849 – 1862.

[3] a) E. Braun, Y. Eichen, U. Sivan, G. Ben-Yoseph, *Nature* **1998**, *391*, 775 – 778; b) K. Keren, M. Krueger, R. Gilad, G. Ben-Yoseph, U. Sivan, E. Braun, *Science* **2002**, *297*, 72 – 75.

[4] Examples: R. K. Soong, G. D. Bachand, H. P. Neves, A. G. Olkhovets, H. G. Craighead, C. D. Montemagno, *Science* **2000**, *290*, 1555 – 1558; G. D. Bachand, R. K. Soong, H. P. Neves, A. G. Olkhovets, H. G. Craighead, C. D. Montemagno, *Nano Lett.* **2001**, *1*, 42 – 45; M. Fischer, A. Bacher, I. Haase, M. Tristl, E. Sackmann, *ChemPhysChem* **2001**, *2*, 623 – 627; for the exploitation of single-molecule biomechanics with optical methods, see A. D. Mehta, M. R. Rief, J. A. Spudich, D. A. Smith, R. M. Simmons, *Science* **1999**, *283*, 1689 – 1695, and references therein; proton pumps, in particular bacteriorhodopsin and ATP synthases, are capable of continuous conversion of light into chemical, mechanical, or electrical energy, which can be used in macro- and nanometer-scale devices: J. K. Lanyi, A. Pohorille, *Trends Biotechnol.* **2001**, *19*, 140 – 144.

[5] N. C. Seeman, *Trends Biotechnol.* **1999**, *17*, 437 – 443.

[6] C. M. Niemeyer, *Chem. Eur. J.* **2001**, *7*, 3188 – 3195.

[7] K. Matsuura, M. Hibino, Y. Yamada, K. Kobayashi, *J. Am. Chem. Soc* **2001**, *123*, 357 – 358.

[8] S. M. Waybright, C. P. Singleton, K. Wachter, C. J. Murphy, U. H. F. Bunz, *J. Am. Chem. Soc* **2001**, *123*, 1828 – 1833.

[9] D. Summerer, A. Marx, *Angew. Chem.* **2002**, *114*, 93 – 95; *Angew. Chem. Int. Ed.* **2002**, *41*, 89 – 90; .

[10] K. Yoshikawa, Y. Matsuzawa, K. Minagawa, M. Doi, M. Matsumoto, *Biochem. Biophys. Res. Commun.* **1992**, *188*, 1274 – 1279.

[11] X. Yang, A. V. Vologodskii, B. Liu, B. Kemper, N. C. Seeman, *Biopolymers* **1998**, *45*, 69 – 83.

[12] C. Mao, W. Sun, Z. Shen, N. C. Seeman, *Nature* **1999**, *397*, 144 – 146.

[13] C. M. Niemeyer, M. Adler, S. Lenhert, S. Gao, H. Fuchs, L. F. Chi, *ChemBioChem* **2001**, *2*, 260 – 265.

[14] Allosteric ribozymes and aptamers, namely designed DNA or RNA nucleic acid motifs which either attain or lose their functionality upon binding of small effector molecules, might also be considered as nanomechanical devices; examples: R. R. Breaker, *Curr. Opin. Biotechnol.* **2002**, *13*, 31 – 39; D. Y. Wang, B. H. Lai, A. R. Feldman, D. Sen, *Nucleic Acids Res.* **2002**, *30*, 1735 – 1742; S. Seetharaman, M. Zivarts, N. Sudarsan, R. R. Breaker, *Nat Biotechnol.* **2001**, *19*, 336 – 341.

[15] S. Tyagi, F. R. Kramer, *Nat. Biotechnol.* **1996**, *14*, 303 – 308.

[16] W. Tan, X. Fang, J. Li, X. Liu, *Chem. Eur. J.* **2000**, *6*, 1107 – 1111.

[17] B. Dubertret, M. Calame, A. J. Libchaber, *Nat. Biotechnol.* **2001**, *19*, 365 – 370.

[18] K. Hamad-Schifferli, J. J. Schwartz, A. T. Santos, S. Zhang, J. M. Jacobson, *Nature* **2002**, *415*, 152 – 155.

[19] A. Jordan, R. Scholz, P. Wust, H. Fähling, *J. Magn. Magn. Mater.* **1999**, *201*, 413 – 419.

[20] J. Fritz, M. K. Baller, H. P. Lang, H. Rothuizen, P. Vettiger, E. Meyer, H. Guntherodt, C. Gerber, J. K. Gimzewski, *Science* **2000**, *288*, 316 – 318.

[21] G. Wu, R. H. Datar, K. M. Hansen, T. Thundat, R. J. Cote, A. Majumdar, *Nat. Biotechnol.* **2001**, *19*, 856 – 860.

[22] K. M. Hansen, H. F. Ji, G. Wu, R. Datar, R. Cote, A. Majumdar, T. Thundat, *Anal. Chem.* **2001**, *73*, 1567 – 1571.

[23] G. Wu, H. Ji, K. Hansen, T. Thundat, R. Datar, R. Cote, M. F. Hagan, A. K. Chakraborty, A. Majumdar, *Proc. Natl. Acad. Sci. USA* **2001**, *98*, 1560 – 1564.

[24] B. Yurke, A. J. Turberfield, A. P. Mills, Jr., F. C. Simmel, J. L. Neumann, *Nature* **2000**, *406*, 605 – 608.

[25] J. J. Li, W. Tan, *Nano Lett.* **2002**, *2*, 315 – 318.

[26] H. Yan, X. Zhang, Z. Shen, N. C. Seeman, *Nature* **2002**, *415*, 62 – 65.

[27] Y. Benenson, T. Paz-Elizur, R. Adar, E. Keinan, Z. Livneh, E. Shapiro, *Nature* **2001**, *414*, 430 – 434.

  1433-7851/02/4120-3783 $ 20.00+.50/0